ELSEVIER

Journal of Alloys and Compounds 218 (1995) 64–72

Journal of ALLOYS AND COMPOUNDS

Structural studies of $LaNi_4CoD_{6.11}$ and $LaNi_{3.55}Mn_{0.4}Al_{0.3}Co_{0.75}D_{5.57}$ by means of neutron powder diffraction

M. Latroche [a], J. Rodríguez-Carvajal [b,c], A. Percheron-Guégan [a], F. Bourée-Vigneron *,[b]

[a] *Laboratoire de Chimie Métallurgique et de Spectroscopie des Terres Rares, UPR 209, CNRS, 1 Pl. A. Briand, 92195 Meudon Cedex, France*
[b] *Laboratoire Léon Brillouin, CEA-CNRS, CE-Saclay, 91191 Gif sur Yvette Cedex, France*
[c] *Institut Laue–Langevin, 156 X, 38042 Grenoble Cedex, France*

Received 26 July 1994

Abstract

The structural properties of $LaNi_4CoD_{6.11}$ and $LaNi_{3.55}Mn_{0.4}Al_{0.3}Co_{0.75}D_{5.57}$ deuterides have been investigated by means of powder neutron diffraction analysis. The data analysis of $LaNi_4CoD_{6.11}$ deuteride has been performed using a modified Rietveld procedure in order to take into account the anisotropic broadening of the observed diffraction lines. Distribution of Mn, Al and Co substituting atoms on the nickel sublattice and occupancy rate determination of the occupied deuterium sites have been achieved and are compared with those of other single substituted compounds.

Keywords: Neutron powder diffraction; Metal hydrides

1. Introduction

The $LaNi_5$ compound is known to absorb large amounts of hydrogen [1] and therefore has been extensively studied [2,3] as a possible candidate to replace cadmium in Ni–Cd batteries. However, when used as a metal hydride electrode, this alloy exhibits too high an equilibrium pressure and too short a cycle lifetime to be of practical interest in commercial batteries [4]. The capacity loss observed when cycling was commonly attributed to the decomposition of the alloy into $La(OH)_3$ and nickel particles, but it has been shown [5] that remarkable improvements on this matter can be achieved by partial substitution on the nickel sublattice with other elements such as cobalt, manganese or aluminium. On those compounds, derived from parent $LaNi_5$, the substituting nature and rate [6] also involve thermodynamical property modifications of the corresponding hydrides (equilibrium pressure and capacity). Although these substitutions involve a decrease of the storage capacity, several compositions have been studied and the best results were obtained from a mischmetal-based three-substituted compound $MmNi_{3.55}Mn_{0.4}Al_{0.3}Co_{0.75}$ [7,8]. (Use of mischmetal was only for economic purpose, since this rare earth mixture is cheaper than pure lanthanum.) Therefore the knowledge of the crystal structure of these hydrides is of great importance to fully understand the substitution effects on the storage properties.

The intermetallic compound $LaNi_5$ is known to crystallize in the hexagonal structure of CaCu5 type (space group P6/mmm) [9,10]. The structure can be briefly described as a stacking of two different planes: the first one, in $z=0$, containing La (1a) and Ni_I (2c) atoms, the second one, in $z=1/2$, built with only Ni_{II} atoms (3g). According to the nature of the substituent M and to the rate of the substitution x, the M atom can be located either on the Ni_{II} site or on both Ni_I and Ni_{II} sites. This occupancy distribution is closely related to the size (i.e. atomic radius) of the substituting element: the larger atoms occupy mainly the 3g (Ni_{II}) site, where there is more space to fit them. In the same way, the range of substitution x for a given element is dependent on its nature: rather low for elements such as Al or Si ($x<1$) but possibly in the whole range $0<x<5$ for elements close to nickel, such as copper or cobalt [11]. In the case of cobalt, Pirogov et al. [12] and Gurewitz et al. [13] report a preference for the substitution of Ni by Co in the 3g site for low x values instead of the expected random distribution.

* Corresponding author.

SSDI 0925-8388(94)01366/7

Concerning the thermodynamical properties of $LaNi_{5-x}Co_x$ metal hydride, several authors [14,15] report various desorption isotherms for this system. The largest hydrogen absorption capacity (6.6 H mol^{-1}) is observed for $LaNi_5$ ($x=0$) and replacement of Ni by Co reduces the absorption capacity (3.5 H mol^{-1} for $x=5$) for hydrogen pressures lower than 10 atm. In this range, for all x values, two plateau pressures can be observed, except for $LaNi_5$ which exhibits a single plateau of equilibrium ($P_{eq}=3$ atm), between the intermetallic compounds (α phase) and $LaNi_5H_{6.6}$ (β phase). For x values greater than zero, the first plateau exhibits a capacity of about 4 H mol^{-1} and the step between the two plateau regions (difference between the desorption pressures of the two plateaus) decreases as a function of x.

The structure of $LaNi_5H_{6.6}$ hydride has been subject to lot of controversy in the past years. Lartigue and co-workers [16] carefully investigated the structure at different concentrations of D and found evidence for a superstructure leading to a doubling of the c-axis and to a new description of the structure in space group $P6_3mc$ with seven interstitial sites for deuterium. At the same time, Thompson et al. [17] studied an isotopic ^{60}Ni deuteride to enhance the D scattering contribution and confirmed the superstructure leading to a double hexagonal cell. In many cases, the anisotropic broadening of the diffraction lines was overcome by modified Rietveld refinement methods [18,19]. Concerning the $LaNi_{5-x}M_xD_y$ system, structural studies by means of neutron diffraction [20] have shown than in the case of M = Al or Mn, for $x>0.2$, the anisotropic broadening effect observed for $LaNi_5$ disappears and the corresponding deuterides were correctly described in the P6/mmm hexagonal space group using the five site model.

In this paper, we will describe structural investigations on $LaNi_4CoD_{6.11}$ and $LaNi_{3.55}Mn_{0.4}Al_{0.3}Co_{0.75}D_{5.57}$ deuterides. This neutron diffraction study has been performed using the Rietveld method [21]. A special subroutine has been developed in order to take into account the anisotropic broadening effects that were observed for $LaNi_4CoD_{6.11}$. Distribution of the substituting elements (Mn, Al and Co) on the nickel sublattice and the nature and rate of sites occupied by the deuterium atoms will be compared.

2. Experimental details

2.1. Synthesis

The intermetallic samples were prepared by induction melting of the pure components (lanthanum, 99.9%; nickel, 99.99%; manganese, 99.99%; aluminium, 99.99% cobalt 99.99%) under vacuum in a water-cooled copper crucible. The samples were remelted five times to ensure good homogeneity. $LaNi_4Co$ was annealed for 3 h at 1050 °C, whereas $LaNi_{3.55}Mn_{0.4}Al_{0.3}Co_{0.75}$ was annealed for 12 days at 900 °C. Both samples were characterized by metallographic examination and microprobe analysis.

The deuterides were obtained by exposing samples to deuterium gas at room temperature and capacity were measured from pressure variations by a so-called volumetric method. Batches of about 7 g were ground mechanically in an inert gaseous atmosphere and were sieved in powders with a grain size less than 36 μm. After several absorption–desorption cycles to obtain powder with homogeneous particle size, samples were charged for the last cycle in a closed quartz cylindrical container.

2.2. X-ray diffraction

The powder X-ray diffraction analysis of the intermetallic compounds was carried out on a Philips step-by-step θ–2θ goniometer using CuK_α radiation ($\lambda=1.5418$ Å). The diffraction patterns were analysed by a whole pattern fitting procedure using the program FULLPROF [22].

2.3. Neutron diffraction

Neutron diffraction measurements on $LaNi_{3.55}Mn_{0.4}Al_{0.3}Co_{0.75}D_{5.57}$ deuteride were performed at room temperature on the diffractometer D1A at the Laboratoire Léon Brillouin in Saclay. The wavelength was 1.984 Å and pattern was recorded over the angular range $10°<2\theta<159°$ by steps of 0.05°. The important background contribution due to the scattering of the silica tube container was taken into account by linear interpolation between a set of points out of the region of the diffraction lines.

Neutron diffraction measurements on the intermetallic compound $LaNi_4Co$ were performed at room temperature on the diffractometer DN5 of the SILOE reactor at the C.E.N.G. in Grenoble. The wavelength was 2.49 Å and the pattern was recorded in the range $27°<2\theta<107°$ in steps of 0.1°. The structure of this inactivated $LaNi_4Co$ intermetallic compound, for which the sample contribution to the linewidth was negligible, was also analysed using the standard refinement procedure.

Neutron diffraction pattern on $LaNi_4CoD_{6.11}$ deuteride was recorded at room temperature on the diffractometer 3T2 at the Laboratoire Léon Brillouin in Saclay. The wavelength was 1.226 Å and the angular range was $6°<2\theta<125°$ in steps of 0.05°. Examination of the diffraction patterns shows a strong anisotropic broadening of the diffraction lines. Therefore, the fitting procedure was done after writing a special subroutine for the FULLPROF program, taking into account the

particular *hkl* linewidth dependence in the hexagonal case. A detailed description based on the formalism already reported in Ref. [23] is given in the Appendix.

3. Results

3.1. Intermetallic compounds

Metallographic examinations of the intermetallic samples show good homogeneity and no inclusions. Results of microprobe analysis lead to stoichiometries (Table 1) in good agreement with the starting compositions. For both samples, the X-ray powder patterns did not show any extra lines and were successfully indexed in the hexagonal P6/mmm space group. For $LaNi_4Co$, the pattern was refined by the Rietveld method assuming the $CaCu_5$ structure with a random distribution of Co atoms on the 2c and 3g Ni sites. The results of the refinement are summarized in Table 2. No anomalous behaviour can be seen in the halfwidth of the lines, which follows the classical Caglioti function [24]. Since nickel and cobalt are neighbours in the periodic table, it is not possible to distinguish them by means of X-ray diffraction, but their Fermi lengths are quite different ($b_{Ni}=10.3$ F whereas $b_{Co}=2.49$ F) so it was possible by neutron diffraction to refine the Co distribution on the Ni sites. This study has been performed on the neutron diffraction pattern of the $LaNi_4Co$ intermetallic and the results show that the distribution of Co is not random but that 75% is located on the 3g site. Comparison between X-ray and neutron results leads to a large difference in the temperature factors. However, the B values obtained from neutron diffraction must be of rather poor validity if one considers the small Q range (1.442 to 3.815 $Å^{-1}$) of this experiment.

3.2. Deuterides

The intermetallic samples were charged to nominal composition 6.11 D mol^{-1} under 5.02 bar for $LaNi_4Co$ and 5.57 D mol^{-1} under 2.92 bar for $LaNi_{3.55}Mn_{0.4}Al_{0.3}Co_{0.75}$.

The neutron diffraction pattern of $LaNi_4CoD_{6.11}$ shows a single-phase compound with large anisotropic line broadening (Fig. 1) which was, therefore, taken into account in the refinement procedure. According to previous works, two different structural models have been tested. The P6/mmm single cell described by Percheron et al. [20] was first tried assuming that five deuterium sites were involved in the structure. However, the refinement leads to rather unsatisfactory reliability factors ($R_I=7.5\%$) and moreover the total D content estimated from this calculation was 5.34 D mol^{-1} far below the expected value of 6.11 D mol^{-1} from the volumetric method. In fact, the best refinement was obtained in the hexagonal space group $P6_3mc$ with a doubled c-axis. This superstructure, already described for $LaNi_5D_{6.7}$, has been interpreted as a consequence of a structural ordering of deuterium atoms and was mainly deduced from one low-intensity extra line at $d=1.805$ Å (Miller indices 203). In our case, careful examination of the diffraction pattern does not show evidence for this line but calculations show that the expected intensity for this extra line correspond to 2% only of the main line. Due to the large background produced by the silica tube container, the low intensity and the large broadening of extra lines with odd l, the observation of this line is quite difficult. However, the refinement is really improved in the $P6_3mc$ space group when compared with the P6/mmm model. Moreover, the total D content obtained from the occupancy factor refinement is in better agreement (6.12 D mol^{-1}) in the case of the double cell. For metals, occupancy factor were kept fixed to the values deduced from the analysis of the intermetallic compound. Concerning the position parameters of metal atoms, very small deviations are observed in comparison to the ideal one expected from the P6/mmm model (Table 3). The position of the deuterium atoms D1 to D6 were kept constrained ($x_{D2i}=x_{D2i-1}$; $y_{D2i}=2x_{D2i}$; $z_{D2i}=z_{D2i-1}+1/2$) since independent refinement does not lead to improvement and was rather unstable. The D site environments are gathered in Table 4. For D1 and D2, it is worth noting that the site radius is lower than the 0.4 Å limit predicted by Westlake [25] for an occupied site.

The $LaNi_{3.55}Mn_{0.4}Al_{0.3}Co_{0.75}D_{5.57}$ neutron diffraction pattern shows a single-phase compound where all the lines can be indexed in a hexagonal cell with space group P6/mmm (Fig. 2). The cell parameters were found

Table 1
Characterization of intermetallic compounds by microprobe analysis and X-ray diffraction

Intermetallic compounds	Microprobe analysis	Cell parameters P6/mmm space group (Å)
$LaNi_4Co$	$La_{0.995(6)}Ni_{4.027(42)}Co_{0.997(42)}$	$a=5.031(5)$ $c=3.984(4)$
$LaNi_{3.55}Mn_{0.4}Al_{0.3}Co_{0.75}$	$La_{0.991(12)}Ni_{3.577(21)}Mn_{0.407(3)}Al_{0.282(3)}Co_{0.749(12)}$	$a=5.067(5)$ $c=4.043(4)$

Table 2
X-ray and neutron powder diffraction refinement results on $LaNi_4Co$ compound (B: istotropic thermal factor in $Å^2$; N site occupancy)

Space group P6/mmm $LaNi_4Co$			X-ray		Neutron	
			B	N	B	N
La	1a	(0, 0, 0)	1.67(3)	1	0.7(2)	1
Ni1				1.60		1.748(8)
	2c	(1/3, 2/3, 0)	1.47(3)		0.8(3)	
Co1				0.40		0.252(8)
Ni2				2.40		2.252(8)
	3g	(1/2, 0, 1/2)	1.47(3)		0.8(3)	
Co2				0.60		0.748(8)
a (Å)			5.031(5)		5.031(3)	
c (Å)			3.984(4)		3.985(3)	
R_p (%)			6.83		3.34	
R_{wp} (%)			8.89		4.24	
R_I (%)			6.43		6.59	
R_{exp} (%)			5.55		2.59	

to be 5.383(1) Å for a and 4.277(1) Å for c, leading to a volume increase of 19.4% upon deuteration. Examination of the diffraction lines shows that there is no anisotropic broadening as observed for $LaNi_4Co$ deuteride. Therefore, the fitting procedure was done using the standard procedure with no *hkl* dependence of the linewidth on the Bragg reflections. The results of the refinement are gathered in Table 5. The crystallographic structure was successfully refined in the hexagonal cell already described for manganese or aluminium [20,26] substituted compounds and there was no evidence for a doubling of the cell as reported for $LaNi_5D_{6.7}$ or $LaNi_4CoD_{6.1}$ deuterides. Due to the large number of atomic parameters involved in the triple substitution, the possibility of replacing some La atoms by pairs of nickel as previously described was not taken into account in our refinements. Regarding nickel sublattice substitution, refinement of occupancy factors was performed two by two in order to determine the repartition of each substituting atoms between the two possible nickel sites. In all cases, the sum of the occupancy factors for each atom was kept fixed to the value expected from the starting stoichiometry. The distribution of atoms was found to be as follows: aluminium is only present in the $z = 1/2$ plane, whereas manganese and cobalt are distributed on both planes with ratios 18–82% for Mn and 25–75% for Co respectively to the $z = 0$ and $z = 1/2$ positions. Concerning deuterium site occupancies, two crystallographic sites are significantly occupied: the 6m (A2B2) and 12n (AB3) ones with 33% and 22% occupancy factors respectively, which represent 4.62 D or 83% of the total D content. The two other occupied sites are the 12o (AB3) and 4h (B4) ones, but with low filling (5.9% and 5.7% respectively). Refined atomic positions of deuterium atoms are found to be very closed to those observed in related previous studies. From our refine-

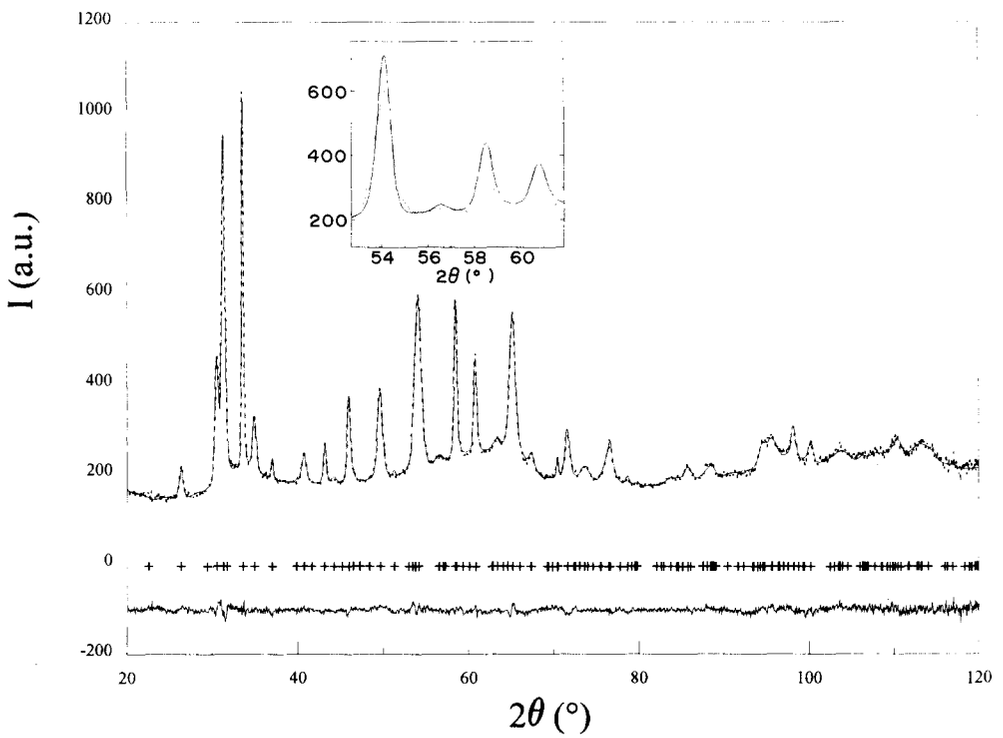

Fig. 1. Observed (...) and calculated (—) neutron diffraction patterns of $LaNi_4CoD_{6.11}$ (difference curve below at the same scale). The inset shows the drastic broadening effect, which cannot be correctly refined when using classical isotropic halfwidth parameters (2θ range: 53° to 62°). Crosses stand for the *hkl* diffraction lines.

Table 3
Atomic and profile parameters for $LaNi_4CoD_{6.11}$ (B: istotropic thermal factor in $Å^2$; N: site occupancy). Profile and strain parameters are described in the Appendix

Atoms		x	y	z	B	N
La	2a	0	0	0.0094(9)	1.23(8)	1
Ni1	2b	1/3	2/3	−0.0055(14)		0.875
Co1						0.125
Ni2	2b	1/3	2/3	0.4965(14)	1.49(3)	0.875
Co2						0.125
Ni3	6c	0.4990(8)	0.5010(8)	1/4		2.25
Co3						0.75
D1	2b	1/3	2/3	0.8076(13)		0.32(3)
D2	2b	1/3	2/3	0.3076(13)		0.31(2)
D3	6c	0.1465(15)	2x	0.25	2.28(9)	1.38(5)
D4	6c	0.1465(15)	2x	0.75		0.49(4)
D5	6c	0.1779(19)	2x	0.3165(18)		0.48(6)
D6	6c	0.1779(19)	2x	0.8165(18)		0.51(6)
D7	12d	0.4683(14)	0	0.0540(3)		2.63(4)

Profile parameters	$U=$ 0.2780	Cell parameters	$a=5.390(1)$ Å
	$V=-0.3450$		$c=8.503(1)$ Å
	$W=$ 0.1480	$\Delta V/V$	22.4%
	$\eta=$ 0.39(1)	D mol^{-1}	6.12(30)
Strain parameters	$S_{AA}=$ 0.562(3)	Reliability factors (%)	$R_p=2.02$ $R_I=4.72$
	$S_{CC}=$ 0.028(2)		$R_{\omega p}=2.42$ $R_{exp}=1.80$
	$C_{AC}=$ 1.000		

Table 4
D site environments for $LaNi_4CoD_{6.11}$. The metal atom radii used for calculations were 1.87 Å for La and the weighted value 1.242 Å for the Ni, Co entity

D atoms		Environment (Å)			Site radius (Å)	Occupancies (%)
D1	2b	1	Ni1	1.589	0.387	16.0%
		3	Ni3	1.640		
D2	2b	1	Ni2	1.606	0.377	15.5%
		3	Ni3	1.623		
D3	6c	1	La	2.595	0.548	23.0%
		1	La	2.461		
		2	Ni3	1.654		
D4	6c	1	La	2.595	0.547	8.2%
		1	La	2.461		
		2	Ni3	1.662		
D5	6c	1	La	2.334	0.437	8.0%
		1	Ni2	2.109		
		2	Ni3	1.604		
D6	6c	1	La	2.334	0.440	8.5%
		1	Ni1	2.096		
		2	Ni3	1.614		
D7	12d	1	La	2.552	0.450	21.9%
		1	Ni1	1.645		
		1	Ni2	1.640		
		1	Ni3	1.675		

ment, there was no evidence for occupancy of the 3f site with A2B4 environment and this site was therefore considered as empty. The total D content deduced from neutron diffraction analysis was estimated to 5.56 ± 0.11 D mol^{-1}, in good agreement with the value measured in the solid–gas experiment.

4. Discussion

The hexagonal structure of $LaNi_5$ is conserved in the intermetallic compound $LaNi_4Co$ and there is no evidence for anisotropy in the width of the diffraction lines. The cobalt atoms are not randomly distributed on the Ni sublattice, but significantly prefer the 3g site. This result is in agreement with that of Gurewitz et al. [14] and with the fact that the 3g site in $z=1/2$ is larger than the 2c site. Since $LaCo_5$ exists and crystallizes also in the $CaCu_5$ structural type, one can expect that for larger x value this ordering phenomenon should progressively disappear.

From the structural study of $LaNi_{3.55}Mn_{0.4}Al_{0.3}Co_{0.75}D_{5.57}$, it has also been possible to study the repartition of substituting atoms on the nickel sublattice. The ratios between the two available sites are in good agreement with those observed for single substituted compounds: the aluminium atom, the largest atom in terms of atomic radius, occupies only the $z=1/2$ plane, as was already observed for $LaNi_{4.6}Al_{0.42}$. Manganese is also preferentially found in this plane, but a small amount (18%) lies in the $z=0$ plane. This value is in fair agreement with the 19% of Mn atoms in $z=0$ observed for $LaNi_{4.76}Mn_{0.32}$ [20]. Finally, cobalt atoms, which are the closest to nickel from the point of view

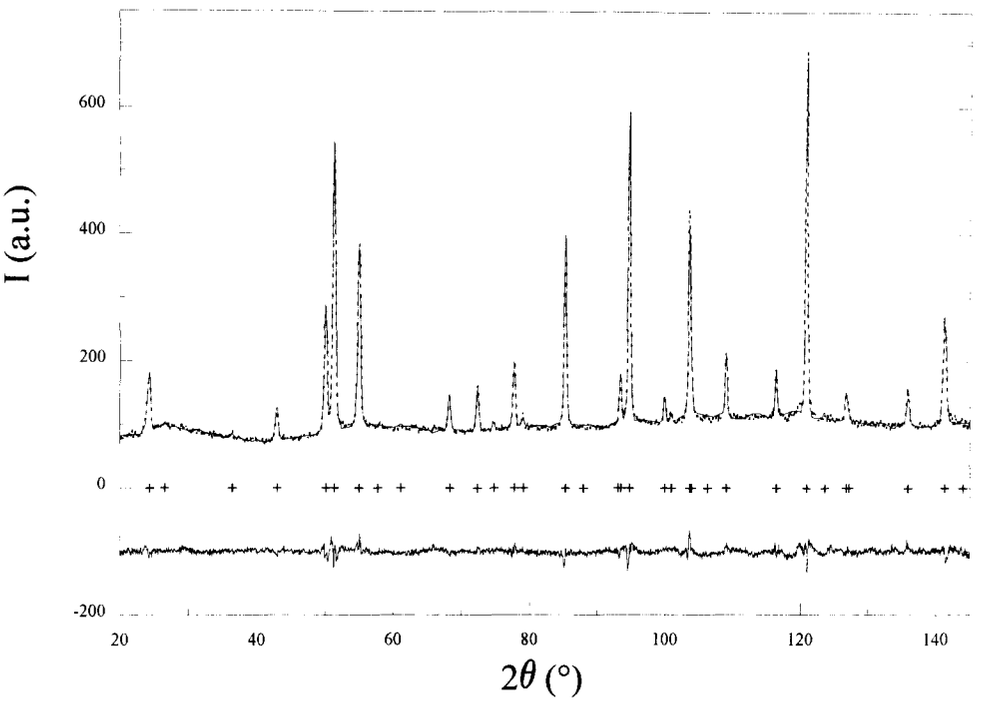

Fig. 2. Observed (...) and calculated (−) neutron diffraction patterns of $LaNi_{3.55}Mn_{0.4}Al_{0.3}Co_{0.75}D_{5.57}$ (difference curve below at the same scale). Crosses stand for the *hkl* diffraction lines.

Table 5
Atomic parameters for $LaNi_{3.55}Mn_{0.4}Al_{0.3}Co_{0.75}D_{5.57}$ (B: isotropic thermal factor in Å^2; N: site occupancy). The metal occupancy factors for Ni, Al, Mn and Co were refined separately assuming a constant sum on the two available sites

Atoms		x	y	z	B	N
La	1a	0	0	0	2.02(7)	1
Ni1	2c					1.736(5)
Mn1					2.09(6)	0.073(15)
Al1		1/3	2/3	0		0.000(39)
Co1						0.188(23)
Ni2	3g					1.813(5)
Mn2						0.326(15)
Al2		1/2	0	1/2	2.08(5)	0.300(39)
Co2						0.561(23)
D1	4h	1/3	2/3	0.3759(64)		0.227(15)
D2	6m	0.1362(09)	2x	1/2	2.76(7)	1.958(31)
D3	12o	0.2234(35)	2x	0.3169(53)		0.712(33)
D4	12n	0.4642(14)	0	0.1004(08)		2.660(30)
Reliability factors (%)		$R_p=3.70$ $R_I=5.56$ $R_{wp}=4.31$		Cell parameters (Å)	$a=5.383(1)$ $c=4.277(1)$	D mol^{-1} 5.56(11)
				$\Delta V/V$	19.4%	

of size but also in terms of electronic properties are found distributed one quarter in the $z=0$ plane and three quarters in the $z=1/2$ plane, in agreement with previous work [14]. From these results, it can be concluded that the atomic repartition for multiple substitutions follows the same geometrical criterion as for single substituted compounds: the largest atoms preferentially occupy the intermediate plane, where there is more space to fit them.

Concerning the deuteride analysis, for $LaNi_4CoD_{6.11}$, compared with other $LaNi_{1-x}M_x$ hydrides, important differences are noted in its behaviour. Whereas in aluminium or manganese compounds, anisotropic broadening of the diffraction lines disappears above $x\sim 0.20$, it remains very important in substituted cobalt compound. The importance of this broadening can be clearly seen in the inset of Fig. 1. This effect attributed to strains upon hydrogenation is described in our refinement through three strain parameters which describe the cell parameter variations S_{AA}, S_{CC} and correlations C_{AC} (cf. Appendix). This latter coefficient was refined and reaches its maximum positive value ($C_{ac}=1$), which means that locally a and c parameters expand (or contract) simultaneously. That is consistent with the nature of the process: interstitial hydrogen atoms that have a tendency to distort locally the occupied sites. From the values of the S_{ij} parameters, one can calculate the microstrain parameters ϵ_a and ϵ_c, which are estimated to $6.12(4)\times10^{-3}$ and $1.01(7)\times10^{-3}$ respectively. It should be pointed out that the ϵ_a/ϵ_c ratio is quite large (6.06), leading to an important anisotropy. It was already observed for $LaNi_5D_{6.7}$ that (001) lines are almost unaffected by broadening, and this effect was attributed to classical faults, such as dislocations locally created by deuteration.

Finally, as was observed in $LaNi_5D_{6.7}$, $LaNi_4CoD_{6.11}$ exhibits a doubling of the cell along the c-axis, which is interpreted as an ordering of deuterium atoms. When

looking at the D occupancy factors, one can see that only D3 and D4 sites exhibit significant differences involving the cell doubling. This relatively small effect explains the weakness of the superstructure lines. However, it was not possible to refine the diffraction pattern correctly without doubling the *c*-axis. All the deuterium sites are significantly occupied, even those with relatively small size like D1 and D2. However, only 0.63 D mol^{-1} are located in these B4 type sites. The remaining D atoms are located for 2.86 D mol^{-1} in the 6c (A2B2+AB3) sites and for 2.63 D mol^{-1} in the 12d (AB3) sites. This repartition is very similar to that observed for $LaNi_5D_y$ except that the ordering of deuterium atoms is less important.

The structural study of $LaNi_{3.55}Mn_{0.4}Al_{0.3}Co_{0.75}D_{5.57}$ shows that this deuteride maintains the P6/mmm hexagonal cell of the parent compound $LaNi_5$. Whereas under hydrogenation $LaNi_5$ and $LaNi_4Co$ deuterides exhibit anisotropic broadening of the diffraction lines attributed to microstrains, this effect is not observed for the three-substituted compound. As has already been pointed out, addition of Mn or Al in single substituted $LaNi_{5-x}M_x$ compounds involves a decrease of microstrains disappearing for $x > 0.2$. The same effect takes place in this case.

Concerning deuterium occupancies, we observed the following site repartition: D2(6m) > D4(12n) > D3(12o) > D1(4h). This repartition is closely related to the site sizes (Table 6) which decrease in the same way. However, if we compare D3(12o) to D4(12n), one can see that the size criterion is not the only effect since their sizes are very similar, whereas occupancy ratios are quite different. In fact, this difference is related to the site environment: both sites are AB3 ones, but whereas for D4 there is only one 3g atom at 1.720 Å involved in the site environment, for D3 there are two of them at 1.577 Å. Since the 3g site located in the $z = 1/2$ plane is richer in aluminium atoms

Table 6
D site environments for $LaNi_{3.55}Mn_{0.4}Al_{0.3}Co_{0.75}D_{5.57}$. The metal atom radii used for calculations were 1.87 Å for La and the weighted values for the Ni, Al, Mn, Co entity were 1.273 Å for the 2c site and 1.245 Å for the 3g one

D atoms		Environment (Å)			Site radius (Å)	Occupancies (%)
D1	4h	1	2c	1.608	0.368	5.6%
		3	3g	1.642		
D2	6m	2	1a	2.487	0.541	32.6%
		2	3g	1.714		
D3	12o	1	1a	2.485		
		1	2c	1.699	0.416	5.9%
		2	3g	1.577		
D4	12n	1	1a	2.535		
		2	2c	1.624	0.439	22.2%
		1	3g	1.720		

Table 7
Comparison of deuterium atomic parameters for single and triple substituted compounds

Single cell *aac* (P6/mmm)	$LaNi_{4.76}Mn_{0.34}D_{6.61}$	$LaNi_{4.60}Al_{0.42}D_{5.4}$	$LaNi_{3.55}Mn_{0.4}Al_{0.3}Co_{0.75}D_{5.56}$	Double cell *aa2c* (P63mc)		$LaNi_4CoD_{6.11}$		$LaNi_5D_{6.7}$	
4h B4 {1/3; 2/3; *z*}	$z = 0.408(4)$	$n = 0.34(2)$	$z = 0.398(8)$	$n = 0.23(2)$	$z = 0.376(6)$	$n = 0.23(2)$	2b {1/3; 2/3; *z*}	B4 {1/3; 2/3; $z+1/2$}	$z = 0.308(1)$ $z' = z+1/2$	$n = 0.31(2)$ $n' = 0.32(3)$	$z = 0.326(6)$ $z' = z+1/2$	$n = 0.08(1)$ $n' = 0.75(7)$
6m A2B2 {*x*; 2*x*; 1/2}	$x = 0.138(1)$	$n = 2.21(3)$	$x = 0.138(1)$	$n = 1.91(3)$	$x = 0.136(1)$	$n = 1.96(3)$	6c {*x*; 2*x*; 1/4}	A2B2 {*x*; 2*x*; 3/4}	$x = 0.146(1)$	$n = 1.38(5)$ $n' = 0.49(4)$	$x = 0.110(8)$	$n = 0.80(15)$ $n' = 0.08(2)$
12n AB3 {*x*; 0; *z*}	$x = 0.466(2)$ $z = 0.102(1)$	$n = 2.78(4)$	$x = 0.470(2)$ $z = 0.103(1)$	$n = 2.62(3)$	$x = 0.464(1)$ $z = 0.100(1)$	$n = 2.66(3)$	12d {*x*; 0; *z*}	AB3	$x = 0.468(1)$ $z = 0.054(1)$	$n = 2.63(4)$	$x = 0.476(10)$ $z = 0.057(2)$	$n = 3.00$
12o AB3 {*x*; 2*x*; *z*}	$x = 0.225(2)$ $z = 0.316(5)$	$n = 1.28(5)$	$x = 0.225(3)$ $z = 0.319(7)$	$n = 0.64(3)$	$x = 0.223(3)$ $z = 0.317(5)$	$n = 0.71(3)$	6c {*x*; 2*x*; *z*}	AB3 {*x*; 2*x*; $z+1/2$}	$x = 0.178(2)$ $z = 0.316(2)$ $z' = z+1/2$	$n = 0.48(6)$ $n' = 0.51(6)$	$x = 0.178(4)$ $z = 0.289(4)$ $z' = z+1/2$	$n = 1.81(15)$ $n' = 0.18(2)$
$\Delta V/V$ (%)	22		19.5		19.4		$\Delta V/V$ (%)	22.4			25.7	

than the 2c site, the lower occupancy factor of D3 can be understood as an electronic effect due to the presence of Al in the $z=1/2$ plane. In the same way, the D1(4h) site of the B4 environment built from three 3g metallic sites is even less occupied. These results agree with previous studies on Al or Mn single-substituted compounds, where the same effects were observed.

Comparison of deuterium atomic parameters for single- and triple-substituted compounds (Table 7) shows that those of $LaNi_{3.55}Mn_{0.4}Al_{0.3}Co_{0.75}D_{5.57}$ are very close to those of $LaNi_{4.6}Al_{0.42}D_{5.4}$. Both compounds exhibit the same occupied sites with roughly the same occupancy factors. The improvement achieved in electrochemical storage capacity by the three-element substitution cannot therefore merely be found in the crystallographic structure of the compound, but should rather be seen in terms of electronic effect. However, it should be pointed out that the three-substituted compound exhibits the smallest volume expansion, which was presented by Willems and Buschow [27] as one of the main criteria for cycle lifetime.

5. Conclusion

In conclusion, it is observed that the behaviour of $LaNi_4Co$ and $LaNi_5$ are very similar. Both compounds crystallize in the $CaCu_5$ type structure and their β phase deuterides exhibit the same anisotropic line broadening and superstructure effects. The ordering effect is less important for the cobalt compound than for $LaNi_5$. The main difference between these two compounds can be seen in the two plateaux isotherm observed for $LaNi_4Co$, but, however, some authors [28,29] also report such behaviour for $LaNi_5$ above 80 °C. It is also worth noting that whereas both $LaNi_5$ and $LaNi_4Co$ deuterides, for higher D content, present deuterium ordering leading to a reduction of symmetry, other substituted compounds with Al or Mn, which do not exhibit anisotropic broadening, can be described in the P6/mmm space group with a single hexagonal cell. From these considerations, we think that an investigation of the structural properties of the deuteride $LaNi_4CoD_4$ should be done in order to determine whether or not microstrains are already induced in this partially charged deuteride. Such a study must help to clarify the role played by deuterium atoms in the deformation process.

The structural study of $LaNi_{3.55}Mn_{0.4}Al_{0.3}Co_{0.75}D_{5.57}$ shows that this three-substituted compound behaves very closely to single-substituted ones in terms of substitution rates. Deuterium atoms occupy the same crystallographic sites as in $LaNi_{4.6}Al_{0.42}D_{5.4}$. The good resistance to corrosion obtained with this compound can be related to the small volume expansion observed during the absorption/desorption process.

Acknowledgements

We are thankful to E. Ressouche from C.E.N.G. in Grenoble for his help in neutron diffraction experiments on $LaNi_4Co$ and to F. Briaucourt, F. Demany and L. Touron from the Laboratoire de Chimie Métallurgique et Spectroscopie des Terres Rares in Meudon for their help in synthesis and analysis of the compounds.

Appendix

The phenomenological model for describing the strains used in this paper follows the method explained in Ref. [23]. The method is based on the assumption that anisotropic microstrains are due to some kind of fluctuations and correlations of the parameters $\{x_i\}$ ($i=1, 2, ..., 6$), where the set $\{x_i\}$ are direct or reciprocal cell parameters, or in general any set of six parameters defining the metrics of the unit cell. The parameters $\{x_i\}$ are considered normally distributed with mean values $\{\alpha_i\}$ and a variance–covariance matrix of components $S_{ij}=\mathrm{cov}(x_i, x_j)[\mathrm{cov}(x_i, x_i)=\sigma^2(\alpha_i)]$ which defines the fluctuations and correlations. The correlation matrix is defined from S_{ij} by $C_{ij}=\mathrm{corr}(x_i, x_j)=\mathrm{cov}(x_i, x_j)/[\sigma(\alpha_i)\sigma(\alpha_j)]$ and have non-diagonal coefficients between -1 and 1. The broadening of Bragg reflections is calculated by applying the propagation error formula to the variable $1/d^2=M(x_i; hkl)$. The mean value of M and its variance are given by:

$$M_{hkl}=M(\alpha_i; hkl) \quad \text{(A1a)}$$

$$\sigma^2(M_{hkl})=\Sigma\Sigma S_{ij}\partial M/\partial\alpha_i \times \partial M/\partial\alpha_j \quad \text{(A1b)}$$

where we have put $\partial M/\partial\alpha_i=(\partial M/\partial x_i)_{x_i=\alpha_i}$. If another set of parameters $p_k=p_k(x_i)$ is used, the relation between their respective covariance matrices is the following:

$$S'_{kn}=(\Sigma_i\Sigma_j\partial p_k/\partial\alpha_i \times S_{ij} \times \partial p_n/\partial\alpha_j) \longrightarrow S'=HSH^{\mathrm{T}} \quad \text{(A2)}$$

The Bragg law allows us to relate the variance of M to the FWHM of the reflection due to strains in the angular space. This strain contribution must be added to the instrumental parameter U in the Caglioti expression in order to obtain the experimental FWMH:

$$H^2=\{U+(8\ \ln\ 2)\sigma^2(M_{hkl})/M^2_{hkl}\}\ \tan^2(\theta)+V\ \tan(\theta)+W \quad \text{(A3)}$$

Let us apply the above formulae to the case of an average hexagonal lattice. We shall use, instead of direct cell parameters, the coefficients of the quadratic form:

$$M_{hkl}=A(h^2+k^2+hk)+Cl^2 \quad \text{(A4)}$$

Using the following notations for the S-matrix components, $\sigma^2(A) = S_{AA}^2$, $\sigma^2(C) = S_{CC}^2$, $\mathrm{cov}(A,C) = C_{AC}$-$(S_{AA}S_{CC})$, the variance of M is obtained by the application of Eqs. (A1) and is given by:

$$\sigma^2(M_{hkl}) = S_{AA}^2(h^2+k^2+hk)^2 + S_{CC}^2 l^4 + 2C_{AC}S_{AA}S_{CC}(h^2+k^2+hk)l^2) \quad \text{(A5)}$$

When using the fluctuations of the coefficients of the quadratic form M_{hkl} one has to interpret what happens in the real space, in terms of fluctuations or direct cell parameters. It is easy to obtain, by applying Eq. (A2), the variance–covariance matrix corresponding to the direct cell parameters as a function of the three parameters S_{AA}, S_{CC} and C_{AC}, which are the actual fitted parameters. The fluctuations and correlation of the direct cell parameters are:

$$\sigma(a) = 3a^3/8 \times S_{AA} \quad \text{(A6a)}$$

$$\sigma(c) = c^3/2 \times S_{CC} \quad \text{(A6b)}$$

$$C_{ac} = C_{AC} \quad \text{(A6c)}$$

An internal multiplicative factor means the fluctuations of A and C are:

$$S_{AA} = 0.562(3) \times 10^{-3}\text{Å}^2 \quad \text{(A7a)}$$

$$S_{CC} = 0.028(2) \times 10^{-3}\text{Å}^2 \quad \text{(A7b)}$$

$$C_{AC} = 1 \quad \text{(A7c)}$$

Then the fluctuations are:

$$\sigma(a) = 3a^3/8 \times S_{AA} = 0.0330(2)\ \text{Å}$$
$$(\epsilon_a = \sigma(a)/a = 6.12(4) \times 10^{-3}) \quad \text{(A8a)}$$

$$\sigma(c) = c^3/2 \times S_{CC} = 0.0086(6)\ \text{Å}$$
$$(\epsilon_c = \sigma(c)/c = 1.01(7) \times 10^{-3}) \quad \text{(A8b)}$$

where ϵ_a and ϵ_c are the microstrain parameters along a and c.

The reader can verify that our formulation, except for an overall isotropic term, is equivalent to that of Ref. [18]. The advantage of our formalism stems from a simpler interpretation of the refined strain parameters. The overall isotropic strain is absorbed in the value of U in Eq. (A3): its expression (when U *is* given in degrees^2) is:

$$[\sigma(M)/M]_{iso} = \pi/180[(U_{ref} - U_{ins})]^{1/2}/(8 \ln 2) \quad \text{(A9a)}$$
$$= 174.53[(U_{ref} - U_{ins})]^{1/2} \quad \text{(A9b)}$$

References

[1] J.H.N. Van Vucht, F.A. Kuijpers and H.C.A.M. Bruning, *Philips Res. Rep., 25* (1970) 133.

[2] G. Bronoël, J. Sarradin, M. Bonnemay, A. Percheron-Guégan, J.C. Achard and L. Schlapbach, *Int. J. Hydrogen Energy, 1* (1976) 251.

[3] A. Percheron-Guégan, J.C. Achard, J. Sarradin and G. Bronoël, in A.F. Andersen and A.J. Maeland (eds.), *Proc. Int. Symp. Hydrides for Energy Storage*, Geilo, Norway, Pergamon, Oxford, 1978, 485.

[4] H.F. Bittner and C.C. Badcock, *J. Electrochem. Soc., 130* (1983) 193C.

[5] J.J.G. Willems, *Philips J. Res., 39* (1) (1984).

[6] H.H. Van Mal, K.H.J. Buschow and A.R. Miedema, *J. Less-Common Met., 35* (1974) 65.

[7] H. Ogawa, M. Ikoma, H. Kawano and I. Matsumoto, *Power Sources, 12* (1988) 393.

[8] M. Ikoma, H. Kawano, I. Matsumoto and N. Yanagihara, *Eur. Patent Appl. No. 0 271 043* (1987).

[9] A. Furrer, P. Fischer, W. Hälg and L. Schlapbach, *Proc. Int. Symp. Hydrides for Energy Storage*, 1977 (1978) 73.

[10] H. Nowotny, *Z. Metallkd., 34* (1942) 247.

[11] A. Percheron-Guégan, C. Lartigue and J.C. Achard, *J. Less-Common Met., 109* (1985) 287 and references therein.

[12] A.N. Pirogov, A.S. Yermolenko, V.N. Dvinyaninov, V.V. Chuyev and V.V. Kelarev, *Phys. Met. Metall., 49* (1980) 120.

[13] E. Gurewitz, H. Pinto, M.P. Dariel and H. Shaked, *J. Phys. F, 13* (1983) 545.

[14] H.H. Van Mal, K.H.J. Buschow and F.A. Kuijpers, *J. Less-Common Met., 32* (1973) 289–296.

[15] C. Colinet, A. Pasturel, A. Percheron-Guégan and J.C. Achard, *J. Less-Common Met., 134* (1987) 109.

[16] C. Lartigue, A. Percheron-Guégan, J.C. Achard and J.L. Soubeyroux, *J. Less-Common Met., 113* (1985) 127.

[17] P. Thompson, J.J. Reilly, L.M. Corliss, J.M. Hastings and R. Hempelmann, *J. Phys. F: Metal Phys., 16* (1986) 675.

[18] P. Thompson, J.J. Reilly and J.M. Hastings, *J. Less-Common Met., 129* (1987) 105.

[19] C. Lartigue, A. Le Bail and A. Percheron-Guégan, *J. Less-Common Met., 129* (1987) 65.

[20] A. Percheron-Guégan, C. Lartigue and J.C. Achard, P. Germi and F. Tasset, *J. Less-Common Met., 74* (1980) 1.

[21] H.M. Rietveld, *Acta Crystallogr., 22* (1967) 151.

[22] J. Rodríguez-Carvajal, *Abstracts of Satellite Meeting on Powder Diffraction*, Congr. Int. Union of Crystallography, Toulouse, France, 1990, p. 127.

[23] J. Rodríguez-Carvajal, M.T. Fernández-Díaz and J.L. Martínez, *J. Phys.: Cond. Matter, 3* (1991) 3215.

[24] G. Caglioti, A. Paoletti and F.P. Ricci, *Nucl. Instrum., 3* (1958) 223.

[25] D.G. Westlake, *J. Less-Common Met., 90* (1983) 251.

[26] J.C.Achard, A.J. Dianoux, C. Lartigue, A. Percheron-Guégan and F. Tasset, in G.J. McCarthy, J.J. Rhyne and H.B. Silver (eds.), *The Rare Earths in Modern Science and Technology*, Vol. 3, Plenum, New York, 1982, p. 481.

[27] J.J.G. Willems and K.H.J. Buschow, *J. Less-Common Met., 129* (1987) 13.

[28] S. Ono, K. Nomura, E. Akiba and H. Uruno, *J. Less-Common Met., 113* (1985) 113–117.

[29] P. Selvam and K. Yvon, *J. Less-Common Met., 171* (1991) L17–L21.